

Research Paper

Mechanistic Approaches to Volume of Distribution Predictions: Understanding the Processes

Trudy Rodgers^{1,2} and Malcolm Rowland¹

Received November 3, 2006; accepted December 8, 2006; published online March 20, 2007

Purpose. To use recently developed mechanistic equations to predict tissue-to-plasma water partition coefficients (K_{pu}), apply these predictions to whole body unbound volume of distribution at steady state ($V_{u,ss}$) determinations, and explain the differences in the extent of drug distribution both within and across the various compound classes.

Materials and Methods. $V_{u,ss}$ values were predicted for 92 structurally diverse compounds in rats and 140 in humans by two approaches. The first approach incorporated K_{pu} values predicted for 13 tissues whereas the second was restricted to muscle.

Results. The prediction accuracy was good for both approaches in rats and humans, with 64–78% and 82–92% of the predicted $V_{u,ss}$ values agreeing with *in vivo* data to within factors of ± 2 and 3, respectively.

Conclusions. Generic distribution processes were identified as lipid partitioning and dissolution where the former is higher for lipophilic unionised drugs. In addition, electrostatic interactions with acidic phospholipids can predominate for ionised bases when affinities (reflected by binding to constituents within blood) are high. For acidic drugs albumin binding dominates when plasma protein binding is high. This ability to explain drug distribution and link it to physicochemical properties can help guide the compound selection process.

KEY WORDS: *in silico* modelling; pharmacokinetics; physicochemical properties; physiological model; tissue distribution.

INTRODUCTION

Two parameters frequently quoted as measures of the extent of drug distribution within the body are the apparent and steady-state volumes of distribution (V and V_{ss} , respectively). The difference between these parameters is that V , estimated during the terminal phase after intravenous drug administration, is influenced by the relative speeds of distribution and elimination, whereas V_{ss} is a much purer distributional term (1), and forms the focus of this research. Conventional methods for determining V_{ss} involve intravenous drug administration followed by compartmental or statistical moment analysis of plasma concentration-time data, or computations from drug affinities for various tissues and organs of the body along with associated tissue and plasma volumes. The latter is implemented less frequently due to the immense time, resource and cost requirements associated with experimentally determining tissue affinities, along with the need for post-dose excision or biopsy from multiple tissues/organs, which raises ethical issues, especially for humans and large animals.

Gaining an insight into the whole body distribution of drugs prior to dose administration would help guide drug candidate selection and assist decision making in drug discovery. Several empirical and semi-empirical approaches have been investigated for predicting drug distribution (2–8) but these require *in vivo* data compilation for regression analysis against physicochemical compound properties, and distributional information cannot be subsequently gained from inaccurate predictions.

Alternative mechanism-based methods however are informative for both inliers and outliers. They are developed from an understanding of the underlying distribution mechanisms along with physiological information and create the potential for *a priori* predictions, as detailed by Davis and Mapleson (9). Such methodologies were later refined and investigated by Poulin *et al.* who developed mechanistic equations to predict the affinity of drugs for various tissues and organs (10,11), which subsequently permitted V_{ss} predictions (12). However, the equations used for these tissue affinity predictions were originally developed for small neutral molecules so when applied to substantially ionised compounds, which comprise many drug substances at physiologic pH, significant inaccuracies were attained. More recently, alternative equations have been developed for predicting tissue-to-plasma water partition coefficients (K_{pu}) that incorporate drug ionisation and provide a more detailed and informative insight into tissue distribution of such compounds (13,14). Using these newer equations

¹ Centre for Applied Pharmacokinetic Research, School of Pharmacy, University of Manchester, Stopford Building, Oxford Road, Manchester, M13 9PT, UK.

² To whom correspondence should be addressed. (e-mail: trudy.rodgers@manchester.ac.uk)

significant improvements in the accuracy of Kpu predictions over the equations of Poulin *et al.* were observed as such the latter equations were not further investigated in this research.

Briefly, the equations of Rodgers *et al.* are based on the assumption that all drugs will dissolve in intra- and extra-cellular tissue water, and partition into the neutral lipids and neutral phospholipids located within tissue cells. An additional mechanism incorporated for compounds with at least one basic $pK_a \geq 7$ (ionised bases and corresponding zwitterions) is electrostatic interactions with tissue acidic phospholipids. For other drug classes associations with extra-cellular proteins are an essential component, where acids and weakly basic compounds are assumed to bind primarily to albumin, and neutral drugs to lipoproteins (13,14).

The aim of this research was to investigate the utility of these recently developed mechanistic equations for predicting Vu_{ss} values in rats and humans, and the possibility of reducing the number of Kpu inputs to just muscle. In addition, these mechanistic approaches were used to explain the differences in the extent of drug distribution both within and across the various compound classes, i.e. bases, acids and neutrals.

MATERIALS AND METHODS

Vu_{ss} values were estimated by each of two approaches that utilise mechanistically predicted Kpu values. The Kpu equation for compounds with at least one basic $pK_a \geq 7$ (Eq. 1), and that for other compound types (Eq. 2) are shown below, but the reader is referred to the original articles for further details (13,14).

$$Kpu = \left[\left(\frac{1+X \cdot f_{IW}}{1+Y} \right) + f_{EW} + \left(\frac{K_{AP} \cdot [AP]_T \cdot X}{1+Y} \right) + \left(\frac{P \cdot f_{NL} + (0.3P+0.7) \cdot f_{NP}}{1+Y} \right) \right] \quad (1)$$

$$Kpu = \left[\left(\frac{1+X \cdot f_{IW}}{1+Y} \right) + f_{EW} + (K_{PR} \cdot [PR]_T) + \left(\frac{P \cdot f_{NL} + (0.3P+0.7) \cdot f_{NP}}{1+Y} \right) \right] \quad (2)$$

where P is the n-octanol:water partition coefficient for unionised compound for all tissues except adipose (vegetable oil:water); f is the fractional tissue volume; subscripts IW and EW refer to intra- and extra-cellular tissue water, NL and NP to tissue neutral lipids and neutral phospholipids, and AP_T and PR_T to the tissue concentrations of acidic phospholipids and extra-cellular albumin (for acids and weak bases) or

lipoprotein (for neutrals), respectively; K_{AP} and K_{PR} are the affinity constants of the drug for acidic phospholipids and either extra-cellular albumin or lipoprotein, respectively; and terms X, Y and Z account for drug ionisation as shown in Table I.

Values for K_{AP} and K_{PR} can be obtained using Eqs. 3 and 4, respectively, for which negative values can be obtained when the affinity is low due to variability and uncertainty in the input parameters. Under such circumstances the affinity constants should be set to zero.

$$K_{AP} = \left[\frac{Kpu_{BC} - \left(\frac{1+Z}{1+Y} \cdot f_{IW,BC} \right)}{\left(\frac{P \cdot f_{NL,BC} + (0.3P+0.7) \cdot f_{NP,BC}}{1+Y} \right)} \right] \cdot \left(\frac{1+Y}{[AP]_{BC} \cdot Z} \right) \quad (3)$$

$$K_{PR} = \left[\frac{\frac{1}{fu} - 1 - \left(\frac{P \cdot f_{NL,P} + (0.3P+0.7) \cdot f_{NP,P}}{1+Y} \right)}{\left(\frac{P \cdot f_{NL,P} + (0.3P+0.7) \cdot f_{NP,P}}{1+Y} \right)} \right] \cdot \frac{1}{[PR]_P} \quad (4)$$

where subscripts BC and P refer to red blood cells and plasma, respectively; pH_{BC} is the intracellular pH of blood cells for which a value of 7.22 was utilised (13); fu is the fraction of drug unbound in plasma; and Kpu_{BC} can be calculated from fu, the blood-to-plasma concentration ratio (R) and the haematocrit (15).

APPROACH 1 (FROM MULTIPLE TISSUE AFFINITY DATA)

In this first approach, Eqs. 1, 2, 3, 4 were utilised to predict the Kpu values in rats and humans for 13 tissues (adipose, bone, brain, gut, heart, kidney, liver, lung, muscle, pancreas, skin, spleen and thymus) using residual blood adjusted rat tissue composition data (13,14) for both species along with species-specific fu and R values (Tables II, III, IV, V). For most drugs these tissues comprise the majority affecting the overall distribution within the body. The Vu_{ss} values were computed by inserting these predicted Kpus into Eq. 5 and converted into L/kg by dividing by 250 g in rats and 70 kg in humans.

$$Vu_{ss} = \frac{V_P}{fu} + \sum V_{T,i} \cdot Kpu_i \quad (5)$$

where V_P and $V_{T,i}$ are the volumes of plasma and the *i*th tissue, respectively (Table VI), and Kpu_i is the mechanistically predicted Kpu of the *i*th tissue (Eqs. 1, 2, 3, 4).

Table I. Definitions of Terms X, Y and Z in Eqs. 1, 2, 3, 4^a

	X	Y	Z
Monoprotic base	$10^{pK_a - pH_{IW}}$	$10^{pK_a - pH_P}$	$10^{pK_a - pH_{BC}}$
Diprotic base ^b	$10^{pK_{a2} - pH_{IW}} + 10^{pK_{a1} + pK_{a2} - 2pH_{IW}}$	$10^{pK_{a2} - pH_P} + 10^{pK_{a1} + pK_{a2} - 2pH_P}$	$10^{pK_{a2} - pH_{BC}} + 10^{pK_{a1} + pK_{a2} - 2pH_{BC}}$
Monoprotic acid	$10^{pH_{IW} - pK_a}$	$10^{pH_P - pK_a}$	NA
Diprotic acid ^b	$10^{pH_{IW} - pK_{a1}} + 10^{2pH_{IW} - pK_{a1} - pK_{a2}}$	$10^{pH_P - pK_{a1}} + 10^{2pH_P - pK_{a1} - pK_{a2}}$	NA
Zwitterion	$10^{pK_{aBASE} - pH_{IW}} + 10^{pH_{IW} - pK_{aACID}}$	$10^{pK_{aBASE} - pH_P} + 10^{pH_P - pK_{aACID}}$	$10^{pK_{aBASE} - pH_{BC}} + 10^{pH_{BC} - pK_{aACID}}$
Neutral	0	0	NA

^a The pHs of plasma (pH_P), intracellular tissue water (pH_{IW}) and blood cells (pH_{BC}) were taken to be 7.4, 7 and 7.22, respectively (13).

^b In these expressions $pK_{a1} < pK_{a2}$.

NA—not applicable

Table II. Prediction Parameters for Compounds with at Least One Basic $pK_a \geq 7$ in Rats and Humans^a

Compound	LogP	pK_a^c	Human			Rat		
			R	fu	Vu_{ss}^b	R	fu	Vu_{ss}^b
Acebutolol-RS	1.87	9.67	1.39	0.77	$1.60^{f,h}$	—	—	—
Acebutolol-R	1.87	9.67	—	—	—	1.09	0.79	11.81
Acebutolol-S	1.87	9.67	—	—	—	1.01	0.73	12.19
Alprenolol	3.16	9.53	0.76	0.20	13.06	—	—	—
Amitriptyline	4.90	9.40	0.86	0.056	148.2	—	—	—
Atenolol	0.38	9.55	1.11	0.96	1.06	—	—	—
Betaxolol-R	2.59	9.40	—	—	—	2.06	0.53	39.61
Betaxolol-S	2.59	9.40	—	—	—	1.91	0.54	36.58
Biperiden	4.25	8.80	0.95	0.10	118.6	1.19	0.17	82.35
Bisoprolol-R	1.87	9.40	—	—	—	1.36	0.85	8.14
Bisoprolol-S	1.87	9.40	—	—	—	1.36	0.85	7.91
Bupivacaine	3.41	8.13	0.68	0.045	20.01	—	—	—
Caffeine	1.29	10.40	1.04	0.70	$0.96^{f,h}$	—	—	—
Carvedilol	4.19	8.10	0.71	0.025	58.66	—	—	—
Carvedilol-R	4.19	8.10	—	—	—	0.81	0.019	94.22
Carvedilol-S	4.19	8.10	—	—	—	1.01	0.037	90.72
Chlorpheniramine	3.07	9.13	1.34	0.28	11.19	—	—	—
Chlorpromazine	5.42	9.70; 6.40	1.17	0.036	280.7	1.56	0.11	274.5
Clomipramine	5.22	9.38	1.05	0.068	296.3	—	—	—
Clozapine	3.42	7.70; 3.70	0.86	0.050	108.0	—	—	—
Cocaine	2.30	8.66	1.00	0.090	22.22	1.00	0.63	4.84
Desipramine	4.45	10.32	0.96	0.19	105.3^e	—	—	—
Diltiazem	2.67	7.70	1.03	0.20	15.22	0.93	0.22	16.59
Diphenhydramine	3.31	8.98	0.74	0.089	42.02	—	—	—
Disopyramide	2.58	9.40	—	—	—	1.00	0.24	$2.68^{f,h}$
Doxepin	4.01	9.00	1.25	0.19	61.43	—	—	—
Doxorubicin	1.27	8.15	—	—	—	1.91	0.34	$242.6^{e,g}$
Ethambutol	−0.40	9.50; 6.30	1.33	0.84	4.65	—	—	—
Etidocaine	3.45	7.80	0.59	0.060	25.42	—	—	—
Exaprolol	3.68	9.27	—	—	—	1.25	0.54	$110.0^{e,g}$
Fentanyl	4.05	8.99	1.00	0.16	22.75	0.89	0.15	30.49
Haloperidol	3.61	8.48	1.08	0.10	173.7	—	—	—
Imipramine	4.80	9.50	1.07	0.13	114.0	1.67	0.24	66.04
Inaperisone	3.72	9.05	—	—	—	1.88	0.24	26.46
Ketamine	2.65	7.50	1.24	0.77	$2.33^{f,h}$	—	—	—
Ketanserin	3.29	7.31^d	0.70	0.049	75.96	—	—	—
Lidocaine	2.44	8.01	0.87	0.35	2.96	1.27	0.38	6.89
Lorcainide	4.85	9.50	0.77	0.16	39.38	—	—	—
Maprotiline	4.50	10.50	1.70	0.12	358.3	—	—	—
Meperidine	2.72	8.64	1.11	0.38	9.62	—	—	—
Mepivacaine	1.88	7.76	0.91	0.23	5.11	—	—	—
Metoclopramide	2.60	9.30	1.08	0.65	5.23	—	—	—
Methadone	3.93	8.94	0.77	0.13	38.98	1.00	0.25	25.79
Metolazone	1.80	9.70	1.13	0.057	28.41^h	—	—	—
Metoprolol-RS	2.15	9.70	1.14	0.90	3.85	—	—	—
Metoprolol-R	2.15	9.70	—	—	—	1.52	0.80	9.84
Metoprolol-S	2.15	9.70	—	—	—	1.51	0.81	9.55
Mexiletine	2.15	9.00	1.12	0.34	14.63	—	—	—
Morphine	0.89	8.35	1.02	0.71	3.65	—	—	—
Naloxone	2.10	7.90	1.22	0.59	7.29	—	—	—
Nicardipine	4.67	8.60	0.71	0.040	24.84^b	—	—	—
Nicotine	1.17	7.80; 3.04	—	—	—	0.80	0.84	1.17
Nitrofurantoin	−0.47	7.20	0.76	0.39	1.47	—	—	—
Ondansetron	1.92	7.40	0.83	0.28	6.62	—	—	—
Oxprenolol-RS	2.18	9.50	0.64	0.14	6.48	—	—	—
Oxprenolol-R	2.18	9.50	—	—	—	0.75	0.29	9.67
Oxprenolol-S	2.18	9.50	—	—	—	0.80	0.41	9.13
Pentazocine	3.31	8.50	1.07	0.37	13.23	1.55	0.46	16.65
Phencyclidine	4.96	9.40	—	—	—	1.12	0.47	26.70
Pindolol-RS	1.75	8.80	0.81	0.41	3.85	—	—	—
Pindolol-R	1.75	8.80	—	—	—	1.23	0.48	9.00
Pindolol-S	1.75	8.80	—	—	—	1.48	0.78	11.01

Table II. (Continued)

Compound	LogP	pKa ^c	Human			Rat		
			R	fu	Vu _{ss} ^b	R	fu	Vu _{ss} ^b
Prilocaine	2.11	7.90	1.25	0.61	6.09	–	–	–
Procainamide	0.88	9.20	0.98	0.84	2.27	1.00	0.92	1.92
Promethazine	4.96	9.60; 6.50	1.50	0.16	87.50	–	–	–
Propafenone	4.24	9.74	0.70	0.050	72.73	0.96	0.022	172.5
Propranolol-RS	3.65	9.45	0.80	0.11	30.09	–	–	–
Propranolol-R	3.65	9.45	–	–	–	0.77	0.044	42.62
Propranolol-S	3.65	9.45	–	–	–	1.29	0.20	50.67
Quinidine	3.44	10.00; 5.40	0.96	0.17	18.26	1.40	0.33	27.09
Remoxipride	2.10	8.90	0.70	0.20	3.35	1.20	0.74	6.08
Ropivacaine	2.90	8.12	0.69	0.070	7.86	–	–	–
Semtilide	1.36	9.50; 7.60	1.09	0.96	0.79	–	–	–
Sildenafil	2.75	7.60	0.62	0.040	30.00	–	–	–
Sotalol	0.53	9.80; 8.25	1.07	1.00	1.13	–	–	–
Sulpiride	0.57	10.19; 9.01	1.00	1.00	0.85 ^h	–	–	–
Theophylline	0.26	8.71	0.83	0.51	1.08	0.91	0.60	0.95
Timolol	1.91	9.21; 8.80	0.81	0.40	5.04	1.10	0.76	6.84
Tolamolol	2.19	7.94	0.76	0.090	29.52	–	–	–
Trimethoprim	1.01	7.16; 6.60	1.28	0.48	3.68 ^h	–	–	–
Verapamil	3.79	8.50	0.84	0.082	57.42	0.85	0.050	88.00
Enoxacin	0.10	6.10(A); 8.70(B)	–	–	–	0.94	0.66	2.38
Lomefloxacin	–0.30	5.80(A); 9.30(B)	–	–	–	0.96	0.72	1.81
Ofloxacin	–0.39	6.10(A); 8.20(B)	–	–	–	0.92	0.77	2.08
Pefloxacin	1.22	6.30(A); 7.60(B)	–	–	–	0.94	0.80	3.44
Pipemedic acid	–2.15	4.94(A); 7.00(B); 3.47(B)	–	–	–	0.94	0.79	2.93

^a All values, unless otherwise stated, are experimental and taken from the literature (3–6,12,13,16,17,27,29–74). Where multiple values are reported means have been taken.

^b Experimental *in vivo* Vu_{ss} (L/kg) in rats and humans computed from plasma volume of distribution at steady state (V_{ss}) and fu, or in rats only from experimental *in vivo* tissue affinities using Eq. 5, where tissue volumes were adjusted to account for body weight (250 g for a standard rat).

^c Here (A) refers to an acidic pKa and (B) a basic pKa. If no term is stated base is inferred.

^d Experimental values could not be found in the literature so predictions were made using SPARC (26).

^e Vu_{ss} value calculated using approach 1 was under-predicted by > ±4 fold.

^f Vu_{ss} value calculated using approach 1 was over-predicted by > ±4 fold.

^g Vu_{ss} value calculated using approach 2 was under-predicted by > ±4 fold.

^h Vu_{ss} value calculated using approach 2 was over-predicted by > ±4 fold.

APPROACH 2 (USING MUSCLE AFFINITY DATA ONLY)

On examination of *in vivo* experimental muscle Kpu and Vu_{ss} (L/kg) values in rats an interesting trend emerged, namely the two parameters were very similar (Fig. 1). The possibility of simplifying Eq. 5 to include only the muscle Kpu was therefore investigated (Eq. 6), where the muscle Kpu values were predicted using Eqs. 1, 2, 3, 4 in both rats and humans using species-specific tissue composition (Table VII), fu and R data (Tables II to V).

$$Vu_{ss} = \frac{V_P}{fu} + Kpu_{muscle} \cdot \sum_{i=1}^{13} V_i \quad (6)$$

where $\sum_{i=1}^{13} V_i$ is the sum of the volumes of the 13 tissues listed in Table VI, Kpu_{muscle} is the mechanistically predicted muscle Kpu value (Eqs. 1, 2, 3, 4) and the resultant Vu_{ss} was body weight normalised by dividing by 250 g for rats and 70 kg for humans.

APPLICATION

Both approaches were used to predict the Vu_{ss} for 92 compounds in rats and 140 compounds in humans. The accuracy of the predictions (Table VIII) was assessed by computing the percentage of predicted values agreeing with experimental Vu_{ss} values (Tables II, III, IV, V) to within factors of ±2, 3 and 4, and calculations of the average fold error (afe; Eq. 7) and the root mean square error (rmse; Eq. 8).

$$afe = 10^{\frac{1}{n} \sum \log \left(\frac{\text{predicted}}{\text{experimental}} \right)} \quad (7)$$

$$rmse = \sqrt{\frac{1}{n} \cdot \sum 10^{(\text{predicted} - \text{experimental})^2}} \quad (8)$$

where n is the number of compounds, predicted is the mechanistically predicted Vu_{ss} (approach 1 or 2) and experimental is the *in vivo* Vu_{ss}.

Equation 6 was also used to investigate the sensitivity of these Vu_{ss} predictions to the physicochemical input param-

Table III. Prediction Parameters for Compounds with at Least One Basic $pK_a < 7$ in Rats and Humans^a

Compound	LogP	pK_a^c	Human		Rat	
			fu	Vu_{ss}^b	fu	Vu_{ss}^b
Alfentanil	2.16	6.50	0.077	6.34	0.11	6.41
Alprazolam	2.09	2.40	0.27	2.21	0.35	5.66
Antipyrine	0.63	1.45	0.96	0.63	—	—
Chloramphenicol	1.14	5.50	0.47	2.00	—	—
Chlordiazepoxide	2.44	4.73	0.053	6.48	0.15	9.69
Cimetidine	0.60	6.80	0.80	1.25	—	—
Cytosine arabinoside	−2.31	4.30	0.87	0.75	—	—
Diazepam	2.84	3.38	0.020	52.94	0.14	41.61 ^f
Dipyridamole	2.70	6.40	0.0087	71.46	—	—
Epiroprim	2.89	6.96	0.11	23.82	0.10	47.73 ^f
Ergotamine	2.47	6.40	0.020	135.0 ^{e,f}	—	—
Etomidate	3.05	4.35	0.24	10.31	0.19	21.10
Famotidine	−0.21	6.86	0.82	1.40	—	—
Fluconazole	0.80	1.77	0.89	0.68	—	—
Flunitrazepam	2.06	1.80	—	—	0.25	15.24 ^f
Metronidazole	−0.06	2.56	0.85	0.91	—	—
Mibefradil	3.86	4.80; 5.50	0.0075	405.3	—	—
Midazolam	3.15	6.01	0.037	37.70	0.059	37.73
Nizatidine	−0.43	6.80; 2.10	0.71	1.69	—	—
Omeprazole	2.16	4.00	0.047	7.22	—	—
Pentoxifylline	0.30	0.30	1.00	4.20 ^{e,f}	—	—
Prazosin	1.74	6.82	0.054	11.32	—	—
Trazodone	3.20	6.79 ^d	0.073	13.79	—	—
Triazolam	2.42	2.00	0.13	5.27	0.28	8.00
Ceftazidime	−0.49	2.53(A); 1.90(A); 3.75(B)	—	—	0.10	2.40
Clonazepam	2.41	10.50(A); 2.05(B)	0.15	19.73	—	—
Isoniazid	−0.70	10.80(A); 3.50(B); 1.82(B)	0.98	0.61	—	—
Lorazepam	2.45	12.25(A); 1.30(B)	0.090	17.78	—	—
Lormetazepam	2.20	10.41(A); 0.38(B) ^d	0.12	12.50	—	—
Meloxicam	3.43	4.20(A); 1.10(B)	0.0060	25.00	—	—
Naldixic acid	1.12	5.54(A); 3.26(B)	—	—	0.29	1.31
Nitrazepam	2.24	10.80(A); 3.30(B)	0.14	14.80	—	—
Oxazepam	2.24	11.60(A); 2.03(B)	0.043	18.12	0.15	8.81
Tenoxicam	1.90	5.30(A); 1.01(B)	0.012	13.45	0.017	12.06

^a All values, unless otherwise stated, are experimental and taken from the literature (3–6,12,14,22,27,29,43–46,48–50,57–61,63,75–82). Where multiple values are reported means have been taken.

^b Experimental *in vivo* Vu_{ss} (L/kg) in rats and humans computed from plasma volume of distribution at steady state (V_{ss}) and fu, or in rats only from experimental *in vivo* tissue affinities using Eq. 5, where tissue volumes were adjusted to account for body weight (250 g for a standard rat).

^c Here (A) refers to an acidic pK_a and (B) a basic pK_a . If no term is stated base is inferred.

^d Experimental values could not be found in the literature so predictions were made using SPARC (26).

^e Vu_{ss} value calculated using approach 1 was under-predicted by $> \pm 4$ fold.

^f Vu_{ss} value calculated using approach 2 was under-predicted by $> \pm 4$ fold.

eters, i.e. P, pK_a , fu and R, for hypothetical neutral, acid, weakly basic and moderately-to-strongly basic compounds (MatLab version 7.0.1). The simulations were then correlated with the major distributional processes accommodated by the mechanistic Kpu equations, namely dissolution into tissue water, lipid partitioning, electrostatic interactions with acidic phospholipids and extra-cellular protein binding.

RESULTS

The accuracy of the Vu_{ss} predictions using approaches 1 and 2 are given in Table VIII and illustrated in Figs. 2 and 3. In general the prediction accuracy of both approaches was good with 92 and 89% in rats ($n=92$) and 87 and 82% in humans ($n=140$) of the predicted Vu_{ss} values agreeing with experimental values to within a factor of ± 3 using approaches

1 and 2, respectively. Predictions were also generally unbiased with average fold errors for the entire datasets ranging from 0.74 to 0.94 for both approaches in both species. Additionally, the precision was similar between methods in both species as shown by the rmse values.

DISCUSSION

Recently developed mechanistic Kpu equations (13,14) have been used to predict Vu_{ss} values in both rats and humans via two methods, and the prediction accuracy was similar and good in all cases. Using these equations significant Kpu, and subsequent Vu_{ss} , under or over-predictions inform the researcher that additional mechanisms are involved in the overall distribution of the compound of interest. Such

Table IV. Prediction Parameters for Acidic Drugs in Rats and Humans^a

Compound	LogP	pKa	Human		Rat	
			fu	Vu_{ss}^b	fu	Vu_{ss}^b
Acetaminophen	0.46	9.44	0.90	1.13	0.88	0.76
Acetylcysteine	−0.60	9.50	0.22	1.53	—	—
Acitretin	6.40	5.10	—	—	0.010	357.0
Amobarbital	1.89	7.90	0.45	2.27	0.48	3.04
Ascorbic acid	−1.85	4.45; 11.60	0.76	0.95	—	—
Barbital	0.65	7.95	—	—	1.00	0.57
5-n-alkyl-5-ethyl barbituric acids:	—	—	—	—	—	—
Methyl	0.05	8.11	—	—	1.00	0.57
Ethyl	0.68	7.88	—	—	0.95	0.54
Propyl	0.77	7.77	—	—	0.87	0.64
Butyl	1.73	7.81	—	—	0.61	1.11
Pentyl	2.24	8.00	—	—	0.50	1.48
Hexyl	2.77	7.74	—	—	0.19	4.95
Heptyl	3.28	7.78	—	—	0.066	16.67
Octyl	3.82	7.78	—	—	0.026	53.85
Nonyl	4.07	7.82	—	—	0.0093	204.3
Bumetanide	2.91	4.50	0.0059	20.75	—	—
Cefazolin	0.28	2.33	—	—	0.16	1.41
Cefiximine	3.87	3.73	0.34	0.33	—	—
Cerivastatin	4.65	4.35; 5.80	0.0070	42.86	—	—
Colchicine	1.15	12.35	0.60	8.67 ^c	—	—
Dideoxyinosine	−1.24	9.06	0.96	0.78	0.97	0.52
Entacapone	2.16	4.55	0.020	13.50	—	—
Fenopropfen	3.70	4.50	0.010	14.06	—	—
Fluvastatin	4.85	4.60	0.0079	53.08	—	—
Furosemide	2.32	3.90	0.012	9.08	—	—
Hexobarbital	1.74	8.29	0.53	2.06	0.62	1.13
Hydrocortisone	1.58	5.10	0.15	6.07 ^c	—	—
Ibuprofen	4.06	4.70	0.0061	16.16	—	—
Indomethacin	4.03	4.50	0.12	1.43	—	—
Ketoprofen	2.90	4.52	—	—	0.029	41.03 ^c
Ketorolac	3.49	3.49	0.0080	13.75	—	—
Mephentoin	1.69	8.51	—	—	0.63	2.05
Methohexital	1.72	8.30	0.27	10.61 ^c	—	—
Nicoumalone-R	1.98	4.70	0.020	9.93	—	—
Nicoumalone-S	1.98	4.70	0.018	18.37	—	—
Penicillin	1.64	2.70	—	—	0.15	1.58
Pentobarbital	2.10	8.11	0.46	2.18	0.54	2.41
Phenobarbital	1.59	7.35	0.52	1.09	0.64	1.59
Phenylbutazone	3.16	4.50	0.0090	13.56	0.042	5.62
Phenytoin	2.50	8.32	0.12	5.09	0.19	7.32
Salicylic acid	2.16	2.99	—	—	0.14	1.27
Thiopental	2.93	7.53	0.18	11.46	0.13	7.85
Tolbutamide	2.39	5.29	—	—	0.27	0.70
Tolcapone	3.15	4.79	0.0010	120.0	—	—
Tolfenamic acid	5.20	4.30	0.0030	48.25	—	—
Valproic acid	2.76	4.60	0.099	1.32	0.37	1.78

^a All values, unless otherwise stated, are experimental and taken from the literature (3,4,6,12,14,21,25,27,29,43–46,57,59–63,83–104). Where multiple values are reported means have been taken.

^b Experimental *in vivo* Vu_{ss} (L/kg) in rats and humans computed from plasma volume of distribution at steady state (V_{ss}) and fu, or in rats only from experimental *in vivo* tissue affinities using Eq. 5, where tissue volumes were adjusted to account for body weight (250 g for a standard rat).

^c Experimental values could not be found in the literature so predictions were made using SPARC (26).

^d Vu_{ss} values calculated using approaches 1 and 2 were under-predicted by > ±4 fold.

information gain cannot be obtained from empirically-based approaches to pharmacokinetic predictions.

Situations that can give rise to under or over-predictions of Kpu values are detailed in previous reports (13,14) and include active transport processes, non-linear pharmacokinetics and binding to tissue constituents not accommodated

by the mechanistic equations. If these mechanisms significantly contribute towards drug distribution in the whole body then Vu_{ss} predictions using these equations may also deviate from experimental values. For example, under-predictions of Kpu values manifested into under-predictions of the Vu_{ss} (6 fold in rats) for doxorubicin, a compound which is known to

Table V. Prediction Parameters for Neutral Drugs in Rats and Humans^a

Compound	LogP	Human		Rat	
		fu	Vu_{ss}^b	fu	Vu_{ss}^b
Betamethasone	1.87	0.36	3.67	—	—
2-Butanol	0.61	—	—	1.00	0.73
Cloprednol	1.68	0.16	5.06	—	—
Coumarin	1.39	0.85	1.51	—	—
Cyclophosphamide	0.63	0.85	0.92	—	—
Cyclosporin	2.92	0.066	28.78	0.083	41.33
Dexamethasone	2.18	0.29	3.89	—	—
Digitoxin	1.85	0.064	12.25	—	—
Digoxin	1.23	0.74	9.12 ^c	0.61	2.08
Enprofylline	0.33	0.49	1.04	—	—
Estradiol	3.40	0.015	80.00	—	—
Ethanol	−0.26	1.00	0.54	1.00	0.78
Ethoxybenzamide	0.79	—	—	0.59	0.95
Ethylene glycol	−1.36	—	—	1.00	0.35
Ftorafur	−0.27	—	—	0.78	0.44
Griseofluvin	2.18	0.20	7.00	—	—
Isosorbide dinitrate	1.31	0.64	2.76	—	—
Isosorbide mononitrate	−0.28	0.98	0.95	—	—
Methoxsalen	2.04	0.090	7.56	—	—
Methyprednisolone	1.82	0.23	6.11	—	—
Prednisolone	2.02	0.11	6.29	0.60	2.28
Prednisone	1.34	0.25	3.88	—	—
Propofol	3.79	0.028	176.5	—	—
t-Butyl Alcohol	0.35	—	—	1.00	1.00
Thiopeta	0.53	0.90	0.78	—	—
Toluene	2.69	1.00	15.40	—	—

^a All values, unless otherwise stated, are experimental and taken from the literature (5,6,12,14,27,29,43–46,57,59,61,63,105–109). Where multiple values are reported means have been taken.

^b Experimental *in vivo* Vu_{ss} (L/kg) in rats and humans computed from plasma volume of distribution at steady state (V_{ss}) and fu, or in rats only from experimental *in vivo* tissue affinities using Eq. 5, where tissue volumes were adjusted to account for body weight (250 g for a standard rat).

^c Vu_{ss} values calculated using approaches 1 and 2 were under-predicted by > ±4 fold.

extensively interact with tissue DNA (16,17). A further example is provided by chlorthalidone (data not reported), a basic compound known to have a high affinity for human carbonic anhydrase, an enzyme primarily located in the

cytosolic fraction of red blood cells (18). This enzyme affinity results in an exceptionally high blood-to-plasma concentration ratio (R) of ca30 (18,19) and when incorporated into Eq. 3 results in over-estimations of the affinity constant of chlorthalidone for acidic phospholipids, which translates into significant over-predictions of Kpu and Vu_{ss} of this compound (>50 fold for Vu_{ss} ; i.e. 20 vs >1,000 L/kg).

Distribution into blood cells also contributes towards the whole body volume of distribution (20), but this compartment was not incorporated into the approaches used in this research due to the difficulty in obtaining R values for a large database of structurally diverse compounds. In addition, for many drugs this component is considered to have a minimal contribution towards the Vu_{ss} since, compounds that poorly distribute into tissues are generally not significantly bound to blood cells, and for compounds with avid tissue affinities, with large Vu_{ss} values, the percentage of the Vu_{ss} attributed to blood binding is generally small (volume of blood cells being <2% of body weight). However, some drugs significantly associate with blood cell-specific constituents such as haemoglobin or carbonic anhydrase (18), and if this affinity is high in comparison with other mechanisms then neglecting blood cell binding may cause Vu_{ss} under-predictions. For example, the acidic drug fluvastatin (Table IV) shows minimal intra-cellular tissue distribution but has an R value of 1.85 in humans (21), which deviates from commonly

Table VI. Tissue Volumes Normalised to Body Weight for a Standard 250 g Rat and 70 kg Human^a

Tissue	Tissue volumes	
	Human (L)	Rat (mL)
Plasma	3.15	8.13
Adipose	10.43	10.43
Bone	9.07	16.47
Brain	1.49	1.30
Gut	1.85	11.10
Heart	0.31	1.08
Kidney	0.31	2.85
Liver	2.52	14.67
Lung	0.92	1.53
Muscle	33.89	136.24
Pancreas	0.21	0.94
Skin	5.63	43.69
Spleen	0.20	0.83
Thymus	0.039	0.73

^a Values taken from the literature (110,111,112)

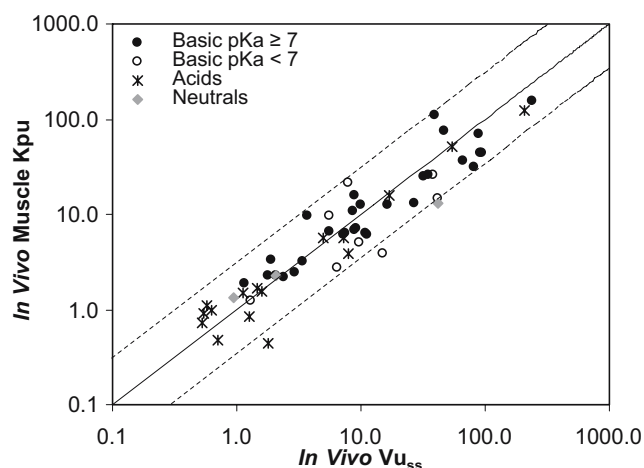


Fig. 1. Correlation between experimental *in vivo* rat muscle Kpu and Vu_{ss} (L/kg) values. The dashed lines represent a factor of three on either side of unity.

observed values for acidic drugs i.e. R close to one minus the haematocrit. Here the Vu_{ss} in humans was under-predicted by a factor of *ca* 3 using Eqs. 5 and 6 but the prediction accuracy was improved to less than a 2 fold deviation from the experimental Vu_{ss} by incorporating a blood cell compartment.

Parameter uncertainty and inherent variability can also influence the accuracy of Kpu predictions as discussed in previous articles (13,14) and this in turn influences the Vu_{ss} prediction accuracy, e.g. tissue composition data uncertainty arising from data compilation from rats of differing ages, strains, weights and gender: experimental difficulties for compounds that are extensively protein bound and/or highly lipophilic: and, the inherent variability associated with all parameters, none of which was explicitly incorporated in the present predictions. An additional factor that can affect Vu_{ss} prediction accuracy is the accuracy of the experimental values to which predictions are compared. As such, to minimize errors, *in vivo* data was only utilised from intravenous studies, since bioavailability introduces uncertainty for other dose routes. Furthermore, all *in vivo* values refer to

steady-state distribution because differences between steady-state and apparent distribution volumes can be pronounced if significant drug elimination has occurred before distribution equilibrium is attained. Despite such care, errors in the *in vivo* Vu_{ss} can still arise that may not be apparent from the published data, e.g. sparse or inappropriate sampling time-points, resulting in imprecise and potentially biased pharmacokinetic calculations. In addition, mean experimental Vu_{ss} values were used for accessing prediction accuracies and for some compounds this average value was derived from data showing pronounced inter-subject or inter-laboratory parameter variability. So when predicted point estimates of the Vu_{ss} are compared with mean *in vivo* data, inaccurate predictions may be inferred but on closer inspection of the experimental data these predictions may fall within the *in vivo* variability boundaries, e.g. in rats the *in vivo* Vu_{ss} reported for flunitrazepam ranged from *ca* 5 to 21 L/kg (22) and whilst the predicted Vu_{ss} was *ca* 5 fold lower than the mean experimental value it was close to the lower limit.

In humans a lack of available tissue composition data necessitated the utilisation of rat information in the 13 tissue approach for human Vu_{ss} predictions. This resulted in good predictions of Vu_{ss} but it is possible that prediction accuracies could be further improved if human tissue composition data were available for a sufficient number of tissues. Such accuracies in the whole body distribution predictions in humans from rat tissue composition information do not automatically infer accurate predictions of the individual tissue Kpu values in humans. In rats accurate tissue Kpu predictions were previously demonstrated across a wide range of structurally diverse compounds by comparing predicted with experimentally determined *in vivo* Kpu values (13,14). Such *in vivo* data in humans are scarce due to ethical issues associated with the requirement for tissue excision/biopsy. The accuracy of mechanistically predicted Kpu values in humans therefore remains uncertain, and it is possible that rat tissue composition data significantly over-predicts the human Kpu's in some tissues and under-predicts it in others resulting in accurate Vu_{ss} predictions due to the errors cancelling each other out. This hypothesis is supported by

Table VII. Muscle, Plasma and Blood Cell Composition Data for Rats and Humans^a

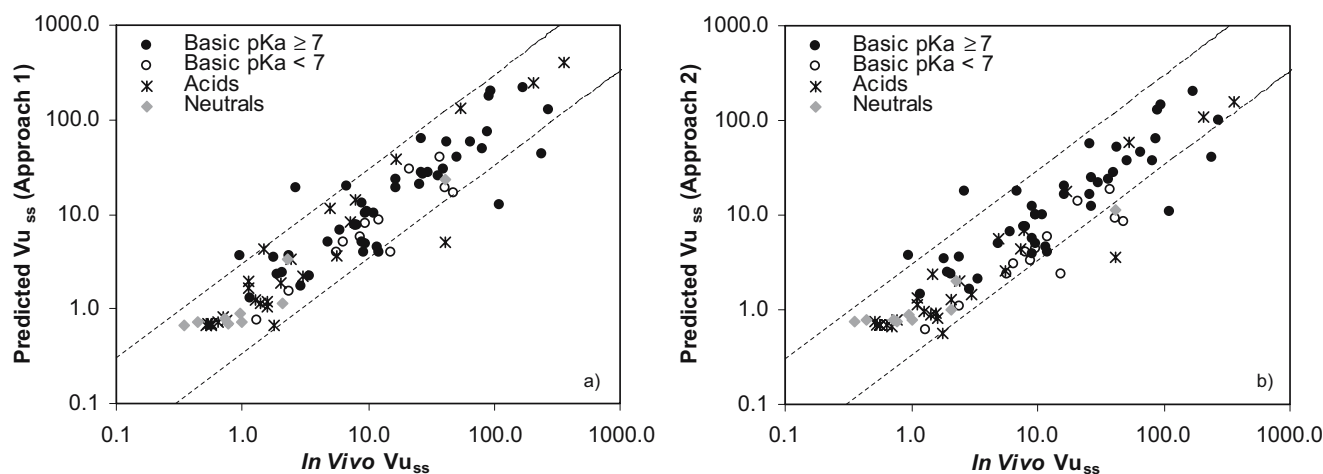
Component	Species	Muscle	Plasma	Blood Cell
Acidic Phospholipids (mg/g)	Human	2.42	0.041	0.57
	Rat	1.50	0.057	0.50
Neutral Phospholipids (fractional volume)	Human	0.0078	0.0021	0.0033
	Rat	0.0072	0.0013	0.0029
Neutral Lipids (fractional volume)	Human	0.022	0.0032	0.0012
	Rat	0.010	0.0023	0.0017
Total Tissue Water (fractional volume)	Human	0.745	0.95	0.63
	Rat	0.726	0.96	0.60
Extra-cellular Water (fractional volume)	Human	0.079	NA	NA
	Rat	0.118	NA	NA
Albumin (tissue to plasma ratio)	Human	0.064 ^b	NA	NA
	Rat	0.064	NA	NA
Lipoprotein (tissue to plasma ratio)	Human	0.059 ^b	NA	NA
	Rat	0.059	NA	NA

^a Values taken from the literature (10,13,14,113–117), where the muscle composition data was adjusted for contributions from residual blood (14).

^b Assumed identical to rat.

Table VIII. Accuracy of the Vuss Predictions Using Approaches 1 (Multiple Tissue Data) and 2 (Muscle Only) in Rats and Humans^a

	Rat		Human	
	Approach 1	Approach 2	Approach 1	Approach 2
Basic pKa ≥ 7	<i>n</i> =43 (Table II)		<i>n</i> =59 (Table II)	
RMSE	46.9	46.1	53.2	47.3
AFE	0.95	0.86	1.10	1.48
% within 2 fold	74.4	72.1	54.2	59.3
% within 2–3 fold	14.0	18.6	27.1	11.9
% within 3–4 fold	4.65	2.33	10.2	18.6
% >4 fold	6.98	6.98	8.47	10.2
Basic pKa<7	<i>n</i> =13 (Table III)		<i>n</i> =31 (Table III)	
RMSE	11.4	15.8	37.5	47.5
AFE	0.66	0.38	0.72	0.68
% within 2 fold	76.9	38.5	64.5	58.1
% within 2–3 fold	15.4	38.5	25.8	35.5
% within 3–4 fold	7.69	0.00	3.23	0.00
% >4 fold	0.00	23.1	6.45	6.45
Acids	<i>n</i> =27 (Table IV)		<i>n</i> =29 (Table IV)	
RMSE	20.3	43.7	8.63	10.3
AFE	1.09	0.75	0.76	0.68
% within 2 fold	77.8	85.2	75.9	72.4
% within 2–3 fold	18.5	7.41	13.8	13.8
% within 3–4 fold	0.00	3.70	0.00	3.45
% >4 fold	3.70	3.70	10.3	10.3
Neutrals	<i>n</i> =9 (Table V)		<i>n</i> =21 (Table V)	
RMSE	6.04	10.0	6.06	8.00
AFE	1.00	0.88	0.64	0.65
% within 2 fold	100	66.7	71.4	71.4
% within 2–3 fold	0.00	22.2	23.8	19.1
% within 3–4 fold	0.00	11.1	0.00	4.76
% >4 fold	0.00	0.00	4.76	4.76
OVERALL	<i>n</i> =92		<i>n</i> =140	
RMSE	34.2	40.0	39.0	38.4
AFE	0.94	0.74	0.86	0.94
% within 2 fold	78.3	70.7	63.6	63.6
% within 2–3 fold	14.1	18.5	23.6	18.6
% within 3–4 fold	3.26	3.26	5.00	9.29
% >4 fold	4.35	7.61	7.86	8.57

^a For RMSE and AFE calculations refer to Eqs. 7 and 8.**Fig. 2.** Comparison of the *in vivo* Vu_{ss} (L/kg) in rats with values predicted using **a** Approach 1 (multiple tissue data) and **b** Approach 2 (muscle only). The dashed lines represent a factor of three on either side of unity.

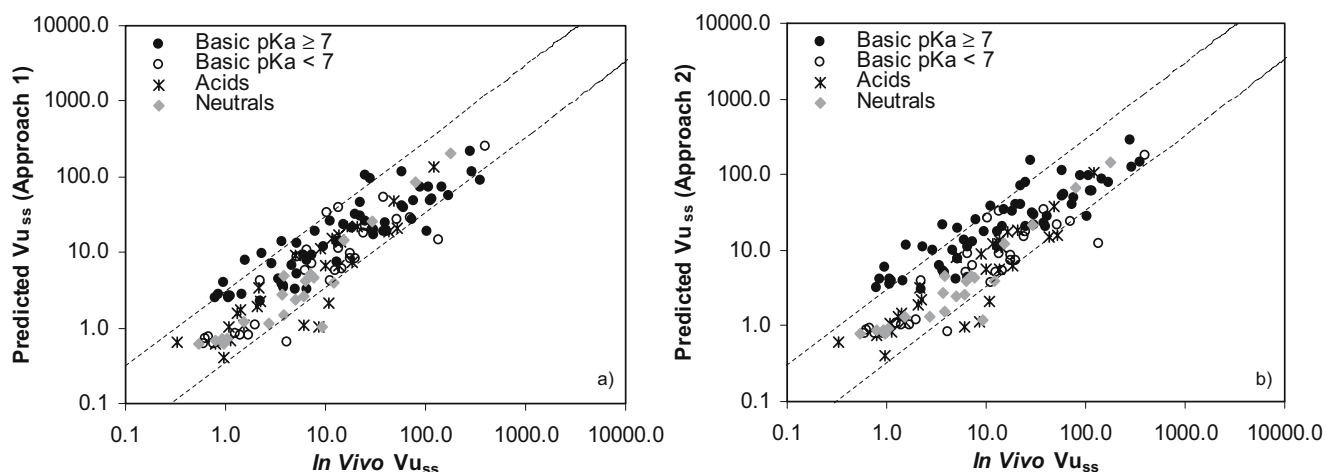


Fig. 3. Comparison of the experimental *in vivo* Vu_{ss} (L/kg) in humans with values predicted using **a** Approach 1 (multiple tissue data) and **b** Approach 2 (muscle only). The *dashed lines* represent a factor of three on either side of unity.

Fig. 4 which indicates that tissue lipid levels may vary across species (differences of up to 7 fold are illustrated). However, uncertainties are associated with these data due to collation from different laboratories where different methods of varying criteria have been employed. If lipid levels are truly different across species then it is highly likely that K_{pu} values may also differ and these differences may be more pronounced for the more lipophilic compounds and for ionised bases. This highlights a need for future experiments to investigate lipid and K_{pu} differences across species for a wide array of compounds and tissues, since such data are currently sparse and hence inconclusive.

The importance of the affinity of drugs for muscle on the whole body volume of distribution is illustrated in Fig. 1, where a good correlation was obtained between experimental muscle K_{pu} and Vu_{ss} values (expressed in L/kg) in rats. This spurred investigations into a simplified approach for Vu_{ss} predictions that used affinity values for muscle as opposed to multiple tissues, and appears to be a novel approach,

although other researchers have alluded to the importance of muscle in the distribution of drugs. For example, good correlations between muscle tissue-to-plasma partition coefficients and those of other tissues have been reported (11,23) and muscle, in combination with adipose, has been shown to represent a significant portion of the whole body steady-state volume of distribution (23).

This good correlation between Vu_{ss} and the muscle K_{pu} (Fig. 1) raises the possibility of predicting the muscle K_{pu} and assuming it to be identical to the Vu_{ss} (L/kg). An assumption of this approach is that the reciprocal of f_u approximates to the muscle K_{pu} , since Eq. 6 simplifies to $Vu_{ss} = K_{pu_{muscle}} \cdot Bodyweight$, but this can lead to inaccuracies for ionised acids since many are avidly associated with albumin and concentrations of this protein are *ca* 20 fold higher in plasma than tissue extra-cellular spaces, which results in $1/f_u \gg$ muscle K_{pu} . Subsequent Vu_{ss} predictions are therefore more accurate for ionised acids when f_u is incorporated (65% (without f_u) vs 81% (including f_u ; Eq. 6)

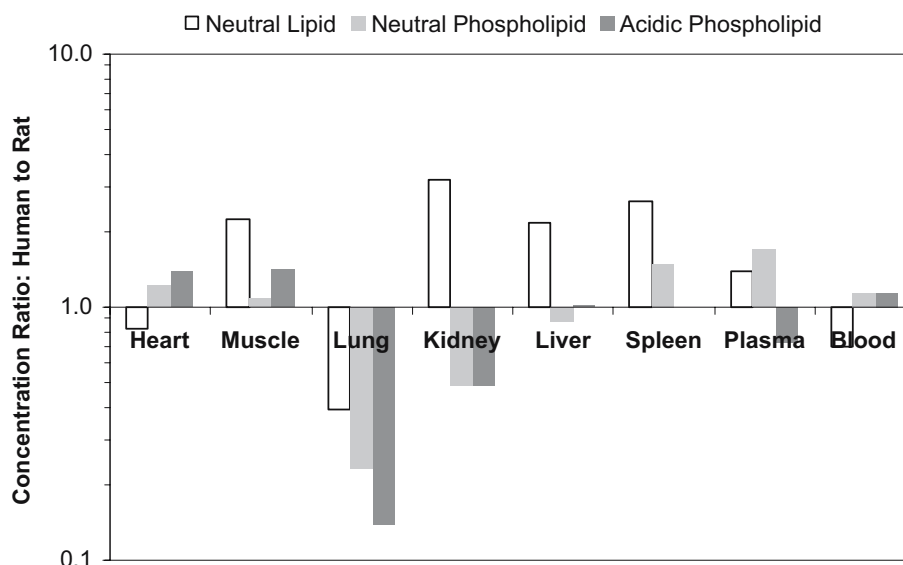


Fig. 4. Ratio of human to rat lipid concentrations in various tissues.

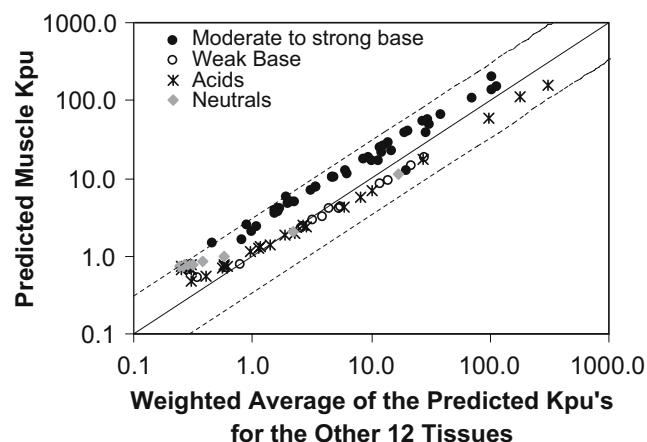


Fig. 5. Correlation between the muscle Kpu and the average of the Kpu values of 12 other tissues in rats^a. ^a Kpu values predicted using Eqs. 1, 2, 3, 4 were used as opposed to experimental data for consistency, since the number of experimental Kpus and tissue types vary across compounds. ^b The weighted average Kpu refers to an adjustment for the contribution of these 12 tissues to body weight, i.e. the weight of these 12 tissues divided by body weight. Such adjustments were not done for muscle since in approach 1 muscle is assumed to account for the distribution into all tissues and organs.

of the predicted $V_{u,ss}$ agreed with experimental values to within a factor of ± 3 based on combined rat and human data ($n=26$)), hence its utility in this research.

Using muscle as the only tissue affinity in $V_{u,ss}$ determinations resulted in good prediction accuracies and the reasons for this are deemed two-fold. Firstly, muscle accounts for a significant proportion of total body weight, namely *ca* 50% (based on a standard 250 g rat and 70 kg human). Secondly, the muscle Kpu on the whole appears to equate to an average of the Kpu values for the other 12 tissues investigated as shown in Fig. 5. An advantage of this muscle approach is that species-specific muscle composition data was used thereby removing inter-species uncertainties, but a disadvantage is that if a drug significantly distributes into a tissue other than muscle then this will not be accommodated

and may lead to under-predictions of $V_{u,ss}$, if it accounts for a significant portion of drug distribution in the whole body.

In this research, predicted Kpu values have been used but experimentally determined *in vitro* data could potentially be utilised for the muscle-only approach since good *in vitro* - *to-in vivo* correlations have been demonstrated by other researchers for this tissue (24,25). A disadvantage of using experimentally determined muscle Kpus is the requirement for muscle tissue, which can be difficult to obtain for humans.

Compound-specific input parameters in the $V_{u,ss}$ predictions were R and f_u , both of which can be determined *in vitro*, and *in silico* LogP and pKa values. In theory, these compound-specific parameters can be estimated before any material is synthesized since software exists for LogP and pKa predictions (26–28), methods are available for f_u predictions (29) and R is commonly assumed to be one for all compounds except ionised acids, where a value of one minus the haematocrit is deemed an appropriate approximation. In practice these predictions and assumptions deviate from the experimental data by varying degrees, and the impact of resultant errors on the mechanistic $V_{u,ss}$ predictions can be seen in Figs. 6, 7, 8, 9.

These simulations show that $V_{u,ss}$ increases exponentially with increasing LogP, so any errors in LogP predictions can significantly influence Kpu and subsequent $V_{u,ss}$ predictions, especially when LogP exceeds 3. An exception is compounds with at least one basic $pK_a \geq 7$ with an avid affinity for acidic phospholipids (Fig. 6), i.e. having a high $K_{pu,BC}$ (function of f_u and R) and low lipid partitioning (function of LogP and pKa). An additional issue for highly lipophilic drugs is the difficulty in accurately quantifying the low drug levels in the aqueous phase, which can result in errors in the experimental LogP determination and in turn cause inaccurate $V_{u,ss}$ predictions. Regarding pKa, the simulations illustrate that $V_{u,ss}$ (and Kpu) values will be significantly influenced by pKa errors for compounds with at least one basic $pK_a \geq 7$ and a low affinity for acidic phospholipids (Fig. 6), along with acidic compounds of pK_a *ca* 6 to 8 (Fig. 7).

Plasma protein binding can also have an exponential influence on $V_{u,ss}$ as demonstrated by Figs. 7, 8, 9, where $V_{u,ss}$ changes more dramatically with f_u when plasma protein

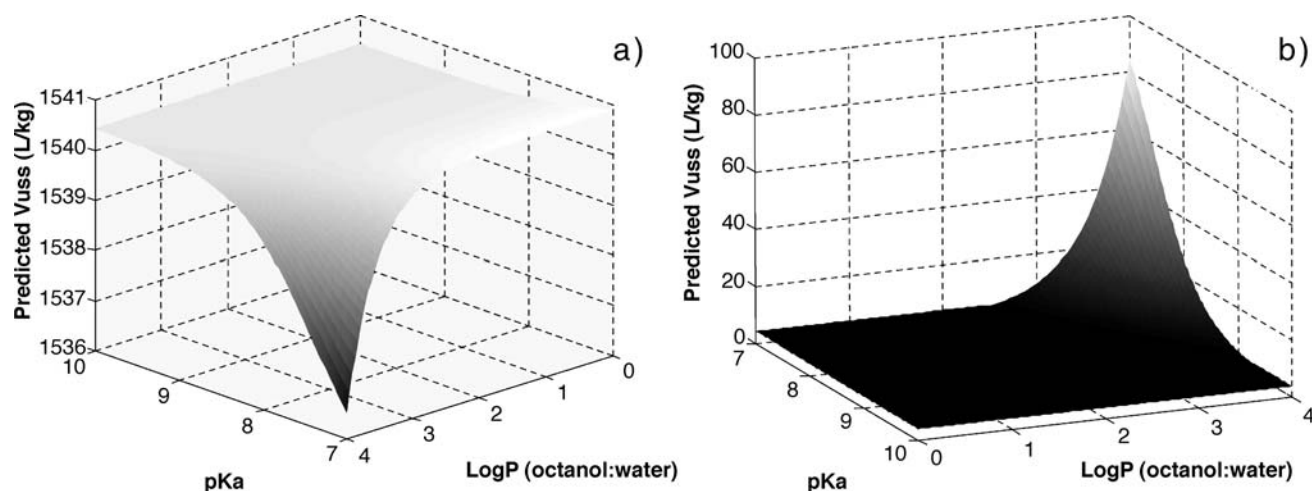


Fig. 6. Simulated influence of LogP (octanol:water) and pKa on $V_{u,ss}$ values (L/kg) predicted using Approach 2 (muscle only) for a monoprotic base, where **a** $f_u=0.01$ and the blood-to-plasma concentration ratio (R)=2, and **b** $f_u=0.1$ and $R=0.6$.

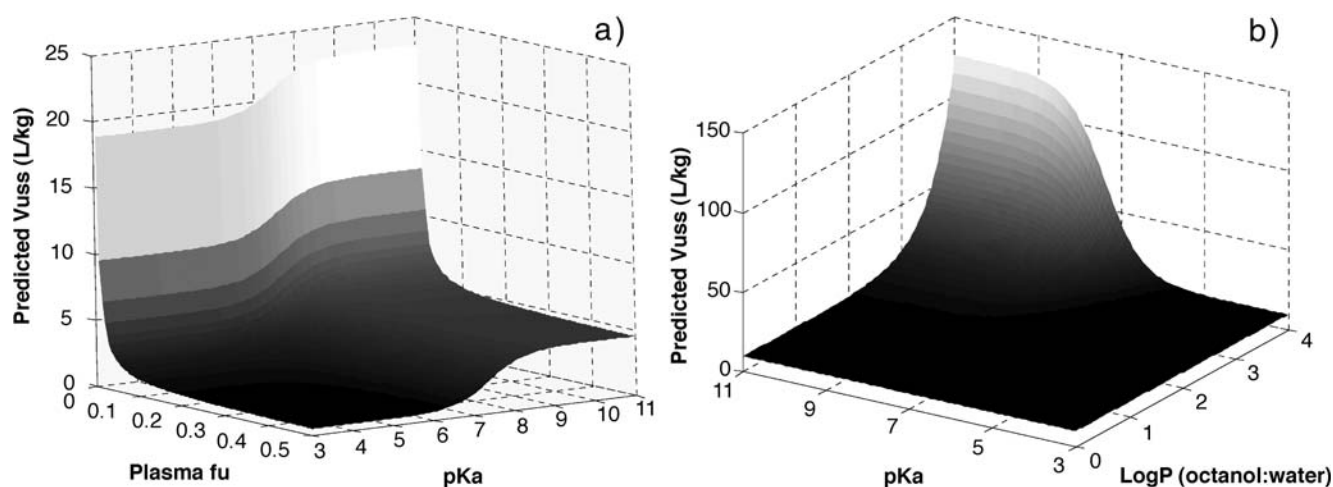


Fig. 7. Simulated influence of **a** plasma f_u and pK_a , where LogP (octanol:water) is set to 2.5, and **b** pK_a and LogP (octanol:water), where $f_u=0.01$ (same trend across f_u), on $V_{u,ss}$ values (L/kg) predicted using Approach 2 (muscle only) for a monoprotic acid.

binding exceeds 90%. The plasma f_u along with R are important in computing the affinity of a compound with at least one basic $pK_a \geq 7$ for tissue acidic phospholipids and, whilst f_u could potentially be predicted, values for R are frequently assumed to be one. This assumption can lead to pronounced errors in acidic phospholipid-drug affinity calcu-

lations and subsequent $V_{u,ss}$ predictions as shown by the linear correlation with R in Fig. 8. Consequently, we recommend against setting R to the arbitrary value of one, but rather it should be determined experimentally.

If the physicochemical property simulations are put into the context of distributional processes the influence of pK_a

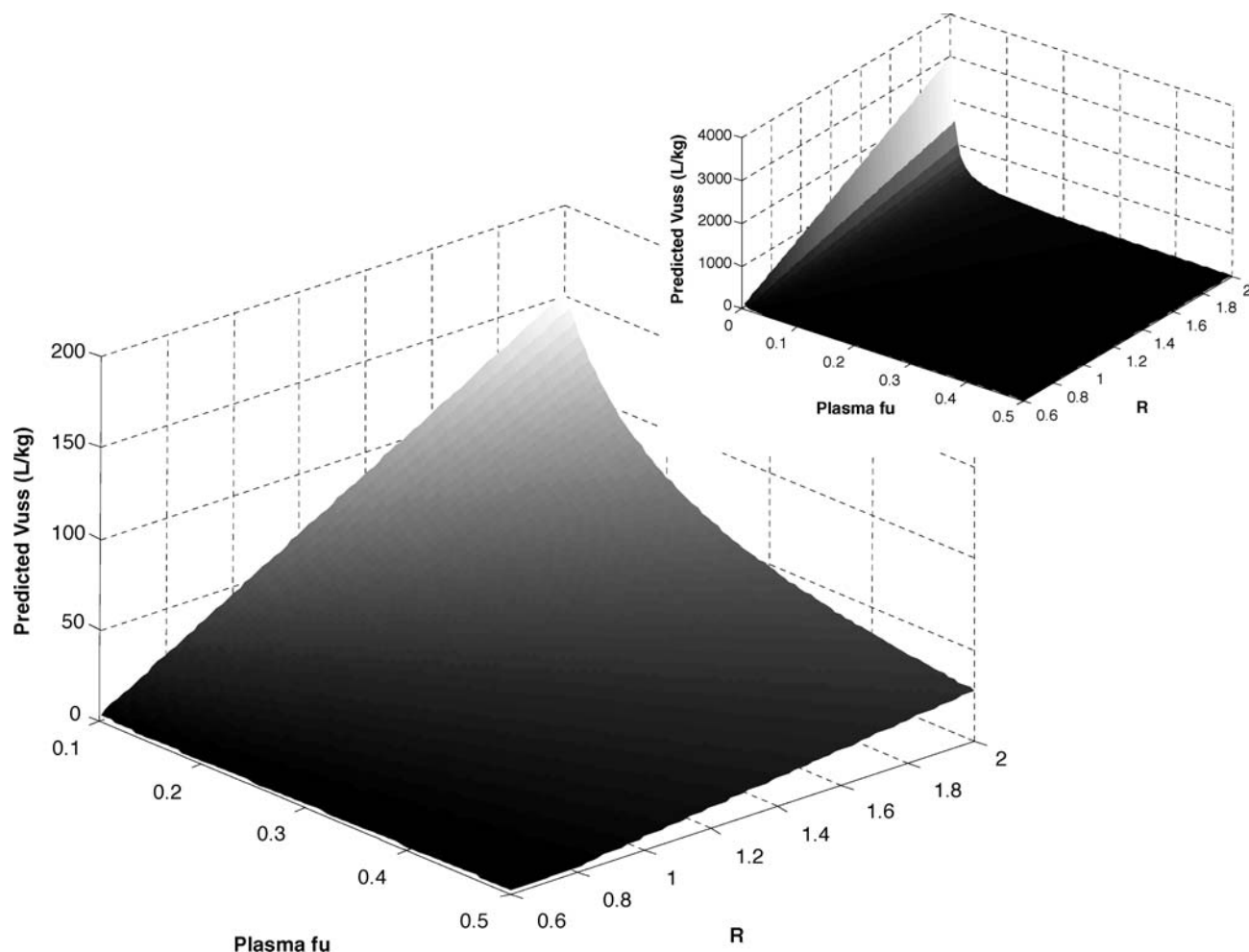


Fig. 8. Simulated influence of plasma f_u and the blood-to-plasma concentration ratio (R) on $V_{u,ss}$ values (L/kg) predicted using Approach 2 (muscle only) for basic drugs, where LogP (octanol:water)=2.5 and $pK_a=9.5$ (expanded f_u range inset).

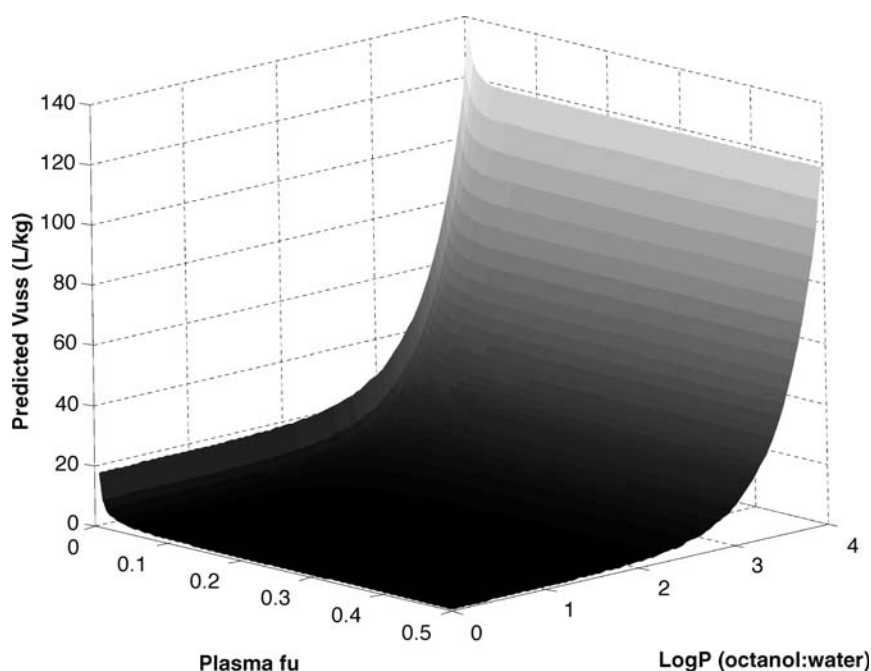


Fig. 9. Simulated influence of LogP (octanol:water) and plasma fu on V_{ss} values (L/kg) predicted using Approach 2 (muscle only) for neutral drugs (same trend for weakly basic drugs).

and LogP on V_{ss} for compounds with at least one basic $pK_a \geq 7$ (Fig. 6) can be attributed to an inter-play between electrostatic interactions with acidic phospholipids, lipid partitioning and dissolution. Namely, when the affinity of a drug for acidic phospholipids is high electrostatic interactions with acidic phospholipids dominate, but at low affinities distribution shifts from a predominance of dissolution for hydrophilic compounds that are primarily ionised at physiological pH to lipid partitioning for hydrophobic drugs that are *ca* 50% ionised within tissue cells. Looking at the simulations for acidic drugs (Fig. 7), the changes in V_{ss} with pK_a and fu can be attributed to lipid partitioning, albumin binding (plasma and the extra-cellular space of tissues) and dissolution. So when an acidic drug is primarily ionised *in vivo* distribution migrates from a predominance of dissolution to one of albumin binding as plasma protein binding increases. However, distribution of unionised acids is primarily dominated by lipid partitioning for lipophilic drugs with low fu's, and by albumin binding for hydrophilic acids that are extensively bound to plasma proteins. For neutral drugs (including weak bases; Fig. 9) increases in LogP translate into increases in the extent of lipid partitioning relative to dissolution, but for hydrophilic compounds binding to extra-cellular proteins (albumin for weak bases and lipoprotein for neutrals) becomes a significant mechanism when fu is less than *ca* 0.05.

While, when testing the ability to predict tissue distribution in humans the only parameters generally available experimentally for most drugs are V_{ss} and Vu_{ss} , these predictions should be placed into perspective with the total objective of physiologically based pharmacokinetics, namely to predict not only the overall extent of distribution, as reflected by V_{ss} and Vu_{ss} , but also the time course of distribution into individual tissues, which is globally manifested in the characteristic polyphasic temporal plasma concentration-time profile after drug administration. Here

the problem is particularly acute when attempting to model events in a tissue with time relative to effects, and when appreciable elimination occurs before distribution equilibrium with tissues is achieved, which violates the assumption that a steady-state approximation exists when characterizing the time course for elimination of drug from the body. Here, information on individual tissue K_{pu} values must be retained and coupled with their respective tissue sizes and blood flows, if we are to meet this higher level objective.

In summary, we have demonstrated that Vu_{ss} values can be predicted from mechanistic determinations of K_{pu} values in either 13 tissues or just muscle, and good prediction accuracies were found for both approaches in rats and humans. In addition, the ability to explain such differences in the extent of tissue distribution for various compounds can help guide compound synthesis and assist decision making in drug discovery, and in general it can be seen that Vu_{ss} values have the ability to be higher for ionised bases.

ACKNOWLEDGEMENTS

Financial support for this project was provided by the following Centre for Applied Pharmacokinetic Research (University of Manchester) Consortium members, Glaxo-SmithKline, Novartis, Pfizer, Servier and Eli Lilly.

REFERENCES

1. M. Rowland and T. N. Tozer. *Clinical pharmacokinetics: concepts and applications*, Chapter 19, Williams & Wilkins, Baltimore, London, 1995.
2. R. A. Herman and P. Veng-Pedersen. Quantitative structure-pharmacokinetic relationships for systemic drug distribution kinetics not confined to a congeneric series. *J. Pharm. Sci.* **83**:423–428 (1994).

3. Y. Sawada, M. Hanano, Y. Sugiyama, H. Harashima, and T. Iga. Prediction of the volumes of distribution of basic drugs in humans based on data from animals. *J. Pharmacokinet. Biopharm.* **12**:587–596 (1984).
4. Y. Sawada, M. Hanano, Y. Sugiyama, and T. Iga. Prediction of the disposition of nine weakly acidic and six weakly basic drugs in humans from pharmacokinetic parameters in rats. *J. Pharmacokinet. Biopharm.* **13**:477–492 (1985).
5. F. Lombardo, R. S. Obach, M. Y. Shalaeva, and F. Gao. Prediction of volume of distribution values in humans for neutral and basic drugs using physicochemical measurements and plasma protein binding data. *J. Med. Chem.* **45**:2867–2876 (2002).
6. F. Lombardo, R. S. Obach, M. Y. Shalaeva, and F. Gao. Prediction of human volume of distribution values for neutral and basic drugs. 2. Extended data set and leave-class-out statistics. *J. Med. Chem.* **47**:1242–1250 (2004).
7. F. Lombardo, R. S. Obach, F. M. Dicapua, G. A. Bakken, J. Lu, D. M. Potter, F. Gao, M. D. Miller, and Y. Zhang. A hybrid mixture discriminant analysis-random forest computational model for the prediction of volume of distribution of drugs in human. *J. Med. Chem.* **49**:2262–2267 (2006).
8. K. W. Ward and B. R. Smith. A comprehensive quantitative and qualitative evaluation of extrapolation of intravenous pharmacokinetic parameters from rat, dog, and monkey to humans. II. Volume of distribution and mean residence time. *Drug Metab. Dispos.* **32**:612–619 (2004).
9. N. R. Davis and W. W. Mapleson. A physiological model for the distribution of injected agents, with special reference to pethidine. *Br. J. Anaesth.* **70**:248–258 (1993).
10. P. Poulin, K. Schoenlein, and F. P. Theil. Prediction of adipose tissue: plasma partition coefficients for structurally unrelated drugs. *J. Pharm. Sci.* **90**:436–447 (2001).
11. P. Poulin and F. P. Theil. A priori prediction of tissue:plasma partition coefficients of drugs to facilitate the use of physiologically-based pharmacokinetic models in drug discovery. *J. Pharm. Sci.* **89**:16–35 (2000).
12. P. Poulin and F. P. Theil. Prediction of pharmacokinetics prior to *in vivo* studies. 1. Mechanism-based prediction of volume of distribution. *J. Pharm. Sci.* **91**:129–156 (2002).
13. T. Rodgers, D. Leahy, and M. Rowland. Physiologically based pharmacokinetic modeling 1: predicting the tissue distribution of moderate-to-strong bases. *J. Pharm. Sci.* **94**:1259–1276 (2005).
14. T. Rodgers and M. Rowland. Physiologically based pharmacokinetic modelling 2: predicting the tissue distribution of acids, very weak bases, neutrals and zwitterions. *J. Pharm. Sci.* **95**:1238–1257 (2006).
15. M. Rowland and T. N. Tozer. *Clinical pharmacokinetics: concepts and applications*. Williams & Wilkins, Baltimore, London, 502–503 (1995).
16. T. Terasaki, T. Iga, Y. Sugiyama, and M. Hanano. Experimental evidence of characteristic tissue distribution of adriamycin. Tissue DNA concentration as a determinant. *J. Pharm. Pharmacol.* **34**:597–600 (1982).
17. T. Terasaki, T. Iga, Y. Sugiyama, and M. Hanano. Pharmacokinetic study on the mechanism of tissue distribution of doxorubicin: interorgan and interspecies variation of tissue-to-plasma partition coefficients in rats, rabbits, and guinea pigs. *J. Pharm. Sci.* **73**:1359–1363 (1984).
18. P. H. Hinderling. Red blood cells: a neglected compartment in pharmacokinetics and pharmacodynamics. *Pharmacol. Rev.* **49**:279–295 (1997).
19. H. L. Fleuren, T. A. Thien, C. P. Verwey-Van Wissen, and J. M. van Rossum. Absolute bioavailability of chlorthalidone in man: a cross-over study after intravenous and oral administration. *Eur. J. Clin. Pharmacol.* **15**:35–50 (1979).
20. H. M. Jones, N. Parrott, K. Jorga, and T. Lave. A novel strategy for physiologically based predictions of human pharmacokinetics. *Clin. Pharmacokinet.* **45**:511–542 (2006).
21. F. L. Tse, D. F. Nickerson, and W. S. Yardley. Binding of fluvastatin to blood cells and plasma proteins. *J. Pharm. Sci.* **82**:942–947 (1993).
22. I. Gueorgieva, I. A. Nestorov, S. Murby, S. Gisbert, B. Collins, K. Dickens, J. Duffy, Z. Hussain, and M. Rowland. Development of a whole body physiologically based model to characterise the pharmacokinetics of benzodiazepines. 1: Estimation of rat tissue-plasma partition ratios. *J. Pharmacokinet. Pharmacodyn.* **31**:269–298 (2004).
23. S. Bjorkman. Prediction of the volume of distribution of a drug: which tissue-plasma partition coefficients are needed? *J. Pharm. Pharmacol.* **54**:1237–1245 (2002).
24. G. Schuhmann, B. Fichtl, and H. Kurz. Prediction of drug distribution *in vivo* on the basis of *in vitro* binding data. *Biopharm. Drug Dispos.* **8**:73–86 (1987).
25. P. Ballard, D. E. Leahy, and M. Rowland. Prediction of *in vivo* tissue distribution from *in vitro* data. 3. Correlation between *in vitro* and *in vivo* tissue distribution of a homologous series of nine 5-n-alkyl-5-ethyl barbituric acids. *Pharm. Res.* **20**:864–872 (2003).
26. SPARC On-Line Calculator. <http://ibmlc2.chem.uga.edu/sparc/>. 29-3-2006.
27. Syracuse Research Corporation: KOWWIN Experimental Database. http://www.syrres.com/esc/est_kowdemo.htm. 29-3-2006.
28. Interactive Analysis. <http://www.logp.com/>. 29-3-2006.
29. K. Yamazaki and M. Kanaoka. Computational prediction of the plasma protein-binding percent of diverse pharmaceutical compounds. *J. Pharm. Sci.* **93**:1480–1494 (2004).
30. P. H. Hinderling, O. Schmidlin, and J. K. Seydel. Quantitative relationships between structure and pharmacokinetics of beta-adrenoceptor blocking-agents in man. *J. Pharmacokinet. Biopharm.* **12**:263–287 (1984).
31. R. Grimaldi, E. Perucca, G. Ruberto, C. Gelmi, F. Trimarchi, M. Hollmann, and A. Crema. Pharmacokinetic and pharmacodynamic studies following the intravenous and oral administration of the antiparkinsonian drug biperiden to normal subjects. *Eur. J. Clin. Pharmacol.* **29**:735–737 (1986).
32. A. G. Burm, A. G. de Boer, J. W. Van Kleef, N. P. Vermeulen, L. G. de Leede, J. Spierdijk, and D. D. Breimer. Pharmacokinetics of lidocaine and bupivacaine and stable isotope labelled analogues: a study in healthy volunteers. *Biopharm. Drug Dispos.* **9**:85–95 (1988).
33. G. T. Tucker and L. E. Mather. Clinical pharmacokinetics of local anaesthetics. *Clin. Pharmacokinet.* **4**:241–278 (1979).
34. M. E. von, K. Reiff, and G. Neugebauer. Pharmacokinetics and bioavailability of carvedilol, a vasodilating beta-blocker. *Eur. J. Clin. Pharmacol.* **33**:511–513 (1987).
35. J. H. Yan, J. W. Hubbard, G. McKay, E. D. Korczynski, and K. K. Midha. Absolute bioavailability and stereoselective pharmacokinetics of doxepin. *Xenobiotica* **32**:615–623 (2002).
36. C. S. Lee, D. C. Brater, J. G. Gambertoglio, and L. Z. Benet. Disposition kinetics of ethambutol in man. *J. Pharmacokinet. Biopharm.* **8**:335–346 (1980).
37. W. J. Tilstone, H. Dargie, E. N. Dargie, H. G. Morgan, and A. C. Kennedy. Pharmacokinetics of metolazone in normal subjects and in patients with cardiac or renal failure. *Clin. Pharmacol. Ther.* **16**:322–329 (1974).
38. M. Guerret, G. Cheymol, M. Hubert, C. Julien-Larose, and D. Lavene. Simultaneous study of the pharmacokinetics of intravenous and oral nicardipine using a stable isotope. *Eur. J. Clin. Pharmacol.* **37**:381–385 (1989).
39. B. Hoener and S. E. Patterson. Nitrofurantoin disposition. *Clin. Pharmacol. Ther.* **29**:808–816 (1981).
40. F. Roila and F. A. Del. Ondansetron clinical pharmacokinetics. *Clin Pharmacokinet.* **29**:95–109 (1995).
41. W. D. Mason and N. Winer. Pharmacokinetics of oxprenolol in normal subjects. *Clin. Pharmacol. Ther.* **20**:401–412 (1976).
42. J. Heykants, P. A. Van, R. Woestenborghs, S. Gould, and J. Mills. Pharmacokinetics of ketanserin and its metabolite ketanserin-ol in man after intravenous, intramuscular and oral administration. *Eur. J. Clin. Pharmacol.* **31**:343–350 (1986).
43. A. C. Moffat, M. D. Osselson, and B. Widdop. *Clarke's analysis of drugs and poisons*, Pharmaceutical, London, 2004.
44. L. S. Goodman, A. Gilman, L. L. Brunton, J. S. Lazo, and K. L. Parker. *Goodman's the pharmacological basis of therapeutics*, McGraw-Hill, New York, 2005.
45. D. B. Jack. *Handbook of clinical pharmacokinetic data*, Macmillan, Basingstoke, Hants, England, 1992.
46. R. S. Obach. Prediction of human clearance of twenty-nine drugs from hepatic microsomal intrinsic clearance data: an examination of *in vitro* half-life approach and nonspecific

- binding to microsomes. *Drug Metab. Dispos.* **27**:1350–1359 (1999).
47. E. Nakashima, K. Yokogawa, F. Ichimura, K. Kurata, H. Kido, N. Yamaguchi, and T. Yamana. A physiologically based pharmacokinetic model for biperiden in animals and its extrapolation to humans. *Chem. Pharm. Bull. (Tokyo)* **35**:718–725 (1987).
48. T. Iwatsubo, N. Hirota, T. Ooie, H. Suzuki, N. Shimada, K. Chiba, T. Ishizaki, C. E. Green, C. A. Tyson, and Y. Sugiyama. Prediction of *in vivo* drug metabolism in the human liver from *in vitro* metabolism data. *Pharmacol. Ther.* **73**:147–171 (1997).
49. Y. Shibata, H. Takahashi, M. Chiba, and Y. Ishii. Prediction of hepatic clearance and availability by cryopreserved human hepatocytes: an application of serum incubation method. *Drug Metab. Dispos.* **30**:892–896 (2002).
50. Y. Naritomi, S. Terashita, S. Kimura, A. Suzuki, A. Kagayama, and Y. Sugiyama. Prediction of human hepatic clearance from *in vivo* animal experiments and *in vitro* metabolic studies with liver microsomes from animals and humans. *Drug Metab. Dispos.* **29**:1316–1324 (2001).
51. H. Komura and M. Iwaki. Nonlinear pharmacokinetics of propafenone in rats and humans: application of a substrate depletion assay using hepatocytes for assessment of nonlinearity. *Drug Metab. Dispos.* **33**:726–732 (2005).
52. A. Somogyi, A. McLean, and B. Heinzow. Cimetidine-procainamide pharmacokinetic interaction in man: evidence of competition for tubular secretion of basic drugs. *Eur. J. Clin. Pharmacol.* **25**:339–345 (1983).
53. J. P. Dubois, W. Kung, W. Theobald, and B. Wirz. Measurement of clomipramine, N-desmethyl-clomipramine, imipramine, and dehydroimipramine in biological fluids by selective ion monitoring, and pharmacokinetics of clomipramine. *Clin. Chem.* **22**:892–897 (1976).
54. National Highway Traffic Safety Administration: Drugs and Human Performance Fact Sheets. <http://www.nhtsa.dot.gov/people/injury/research/job185drugs/technical-page.htm>. 29-3-2006.
55. E. A. Taylor and P. Turner. The distribution of propranolol, pindolol and atenolol between human erythrocytes and plasma. *Br. J. Clin. Pharmacol.* **12**:543–548 (1981).
56. G. J. Muirhead, D. J. Rance, D. K. Walker, and P. Wastall. Comparative human pharmacokinetics and metabolism of single-dose oral and intravenous sildenafil. *Br. J. Clin. Pharmacol.* **53**: Suppl 1 13S–20S (2002).
57. R. P. Austin, P. Barton, S. L. Cockroft, M. C. Wenlock, and R. J. Riley. The influence of nonspecific microsomal binding on apparent intrinsic clearance, and its prediction from physicochemical properties. *Drug Metab. Dispos.* **30**:1497–1503 (2002).
58. R. P. Austin, P. Barton, S. Mohamed, and R. J. Riley. The binding of drugs to hepatocytes and its relationship to physicochemical properties. *Drug Metab. Dispos.* **33**:419–425 (2005).
59. Application Note: Partition Coefficient (LogD). <http://www.cerep.fr/Cerep/Users/pages/Downloads/Documents/Marketing/Pharmacology%20&%20ADME/Application%20notes/partitioncoefficient.pdf>. 29-3-2006.
60. E. A. Kolovanov and A. A. Petrauskas. Re-evaluation of logP data for 22 drugs and comparison of 6 calculation methods. http://www.acdlabs.com/publish/ac_logp.html. 29-3-2006.
61. Y. Zhao, J. Jona, D. T. Chow, H. Rong, D. Semin, X. Xia, R. Zanon, C. Spancake, and E. Maliski. High-throughput logP measurement using parallel liquid chromatography/ultraviolet/mass spectrometry and sample-pooling. *Rapid Commun. Mass Spectrom.* **16**:1548–1555 (2002).
62. P. D. Worboys, A. Bradbury, and J. B. Houston. Kinetics of drug metabolism in rat liver slices. III. Relationship between metabolic clearance and slice uptake rate. *Drug Metab. Dispos.* **25**:460–467 (1997).
63. B. N. Singh. A quantitative approach to probe the dependence and correlation of food-effect with aqueous solubility, dose/solubility ratio, and partition coefficient (Log P) for orally active drugs administered as immediate-release formulations. *Drug Dev. Res.* **65**:55–75 (2005).
64. I. Mahmood and C. Sahajwalla. Clinical pharmacokinetics and pharmacodynamics of buspirone, an anxiolytic drug. *Clin. Pharmacokinet.* **36**:277–287 (1999).
65. C. E. Lin, W. S. Liao, K. H. Chen, and W. Y. Lin. Influence of pH on electrophoretic behavior of phenothiazines and determination of pKa values by capillary zone electrophoresis. *Electrophoresis* **24**:3154–3159 (2003).
66. W. Sorasuchart, J. Wardrop, and J. W. Ayres. Drug release from spray layered and coated drug-containing beads: effects of pH and comparison of different dissolution methods. *Drug Dev. Ind. Pharm.* **25**:1093–1098 (1999).
67. T. Rodgers, D. Leahy, and M. Rowland. Tissue distribution of basic drugs: accounting for enantiomeric, compound and regional differences amongst beta-blocking drugs in rat. *J. Pharm. Sci.* **94**:1237–1248 (2005).
68. M. Fujimaki. Stereoselective disposition and tissue distribution of carvedilol enantiomers in rats. *Chirality* **4**:148–154 (1992).
69. O. Nagata, M. Murata, H. Kato, T. Terasaki, H. Sato, and A. Tsuji. Physiological pharmacokinetics of a new muscle-relaxant, inaperisone, combined with its pharmacological effect on blood flow rate. *Drug Metab. Dispos.* **18**:902–910 (1990).
70. N. Yata, T. Toyoda, T. Murakami, A. Nishiura, and Y. Higashi. Phosphatidylserine as a determinant for the tissue distribution of weakly basic drugs in rats. *Pharm. Res.* **7**:1019–1025 (1990).
71. S. Y. Yu, H. C. Chung, E. J. Kim, S. H. Kim, I. Lee, S. G. Kim, and M. G. Lee. Effects of acute renal failure induced by uranyl nitrate on the pharmacokinetics of intravenous theophylline in rats: the role of CYP2E1 induction in 1,3-dimethyluric acid formation. *J. Pharm. Pharmacol.* **54**:1687–1692 (2002).
72. M. Telting-Diaz, D. O. Scott, and C. E. Lunte. Intravenous microdialysis sampling in awake, freely-moving rats. *Anal. Chem.* **64**:806–810 (1992).
73. E. Okezaki, T. Terasaki, M. Nakamura, O. Nagata, H. Kato, and A. Tsuji. Structure-tissue distribution relationship based on physiological pharmacokinetics for NY-198, a new antimicrobial agent, and the related pyridonecarboxylic acids. *Drug Metab. Dispos.* **16**:865–874 (1988).
74. H. Komura and M. Iwaki. Pharmacokinetics and metabolism of metoprolol and propranolol in the female DA and female Wistar rat: the female DA rat is not always an animal model for poor metabolizers of CYP2D6. *J. Pharm. Sci.* **94**:397–408 (2005).
75. T. D. Bjornsson and C. Mahony. Clinical pharmacokinetics of dipyrindamole. *Thromb Res Suppl.* **4**:93–104 (1983).
76. T. Takabatake, H. Ohta, M. Maekawa, Y. Yamamoto, Y. Ishida, H. Hara, S. Nakamura, Y. Ushio, M. Kawabata, and N. Hashimoto. Pharmacokinetics of famotidine, a new H₂-receptor antagonist, in relation to renal function. *Eur. J. Clin. Pharmacol.* **28**:327–331 (1985).
77. U. Busch, G. Heinzl, and H. Narjes. The effect of cholestyramine on the pharmacokinetics of meloxicam, a new non-steroidal anti-inflammatory drug (NSAID), in man. *Eur. J. Clin. Pharmacol.* **48**:269–272 (1995).
78. N. A. Von, H. J. Huber, and F. Stanislaus. Pharmacokinetics of nilvadipine. *J. Cardiovasc. Pharmacol.* **20**(: Suppl 6): S22–S29 (1992).
79. H. C. Rawden, D. J. Carlile, A. Tindall, D. Hallifax, A. Galetin, K. Ito, and J. B. Houston. Microsomal prediction of *in vivo* clearance and associated interindividual variability of six benzodiazepines in humans. *Xenobiotica* **35**:603–625 (2005).
80. N. Blanchard, E. Alexandre, C. Abadie, T. Lave, B. Heyd, G. Mantion, D. Jaek, L. Richert, and P. Coassolo. Comparison of clearance predictions using primary cultures and suspensions of human hepatocytes. *Xenobiotica* **35**:1–15 (2005).
81. M. S. Islam and M. M. Narurkar. Solubility, stability and ionization behaviour of famotidine. *J. Pharm. Pharmacol.* **45**:682–686 (1993).
82. L. Granero, J. Chesa-Jimenez, F. Torres-Molina, and J. E. Peris. Distribution of ceftazidime in rat tissues. *Biopharm. Drug Dispos.* **19**:473–478 (1998).
83. L. F. Prescott. Kinetics and metabolism of paracetamol and phenacetin. *Br. J. Clin. Pharmacol.* **10**(: Suppl 2): 291S–298S (1980).
84. L. Borgstrom, B. Kagedal, and O. Paulsen. Pharmacokinetics of N-acetylcysteine in man. *Eur. J. Clin. Pharmacol.* **31**:217–222 (1986).
85. H. S. Lau, M. L. Hyneck, R. R. Berardi, R. D. Swartz, and D. E. Smith. Kinetics, dynamics, and bioavailability of bume-

- tanide in healthy subjects and patients with chronic renal failure. *Clin. Pharmacol. Ther.* **39**:635–645 (1986).
86. M. E. Klepser, M. N. Marangos, K. B. Patel, D. P. Nicolau, R. Quintiliani, and C. H. Nightingale. Clinical pharmacokinetics of newer cephalosporins. *Clin. Pharmacokinet.* **28**:361–384 (1995).
87. W. Muck. Clinical pharmacokinetics of cerivastatin. *Clin. Pharmacokinet.* **39**:99–116 (2000).
88. A. Rubin, B. E. Rodda, P. Warrick, A. S. Ridolfo, and C. M. Gruber Jr.. Physiological disposition of fenoprofen in man. II. Plasma and urine pharmacokinetics after oral and intravenous administration. *J. Pharm. Sci.* **61**:739–745 (1972).
89. C. D. Scripture and J. A. Pieper. Clinical pharmacokinetics of fluvastatin. *Clin. Pharmacokinet.* **40**:263–281 (2001).
90. D. E. Smith, E. T. Lin, and L. Z. Benet. Absorption and disposition of furosemide in healthy volunteers, measured with a metabolite-specific assay. *Drug Metab. Dispos.* **8**:337–342 (1980).
91. H. Cheng, J. D. Rogers, J. L. Demetriades, S. D. Holland, J. R. Seibold, and E. Depuy. Pharmacokinetics and bioinversion of ibuprofen enantiomers in humans. *Pharm. Res.* **11**:824–830 (1994).
92. L. Helleberg. Clinical Pharmacokinetics of indomethacin. *Clin. Pharmacokinet.* **6**:245–258 (1981).
93. N. Y. Le, V. C. de, M. Pinaud, J. M. Bernard, J. P. Fraboul, A. Athouel, M. Ribeyrol, N. Beneroso, and C. Larousse. Pharmacokinetics and haemodynamic effects of prolonged methohexitone infusion. *Br. J. Clin. Pharmacol.* **26**:589–594 (1988).
94. D. D. Breimer. Pharmacokinetics of methohexitone following intravenous infusion in humans. *Br. J. Anaesth.* **48**:643–649 (1976).
95. J. Godbillon, J. Richard, A. Gerardin, T. Meinertz, W. Kasper, and E. Jahnchen. Pharmacokinetics of the enantiomers of acenocoumarol in man. *Br. J. Clin. Pharmacol.* **12**:621–629 (1981).
96. R. Gugler, C. V. Manion, and D. L. Azarnoff. Phenytoin: pharmacokinetics and bioavailability. *Clin. Pharmacol. Ther.* **19**:135–142 (1976).
97. K. M. Jorga, B. Fotteler, P. Heizmann, and G. Zurcher. Pharmacokinetics and pharmacodynamics after oral and intravenous administration of tolcapone, a novel adjunct to Parkinson's disease therapy. *Eur. J. Clin. Pharmacol.* **54**:443–447 (1998).
98. P. J. Pentikainen, O. Tokola, E. Alhava, and A. Penttila. Pharmacokinetics of tolfenamic acid: disposition in bile, blood and urine after intravenous administration to man. *Eur. J. Clin. Pharmacol.* **27**:349–354 (1984).
99. R. K. Verbeeck, J. L. Blackburn, and G. R. Loewen. Clinical pharmacokinetics of non-steroidal anti-inflammatory drugs. *Clin. Pharmacokinet.* **8**:297–331 (1983).
100. D. Jung, E. Mroczak, and L. Bynum. Pharmacokinetics of ketorolac tromethamine in humans after intravenous, intramuscular and oral administration. *Eur. J. Clin. Pharmacol.* **35**:423–425 (1988).
101. H. Heikkinen, M. Saraheimo, S. Antila, P. Ottoila, and P. J. Pentikainen. Pharmacokinetics of entacapone, a peripherally acting catechol-O-methyltransferase inhibitor, in man. A study using a stable isotope technique. *Eur. J. Clin. Pharmacol.* **56**:821–826 (2001).
102. T. B. Andersson, E. Bredberg, H. Ericsson, and H. Sjoberg. An evaluation of the *in vitro* metabolism data for predicting the clearance and drug-drug interaction potential of CYP2C9 substrates. *Drug Metab. Dispos.* **32**:715–721 (2004).
103. D. W. Boulton, U. K. Walle, and T. Walle. Extensive binding of the bioflavonoid quercetin to human plasma proteins. *J. Pharm. Pharmacol.* **50**:243–249 (1998).
104. L. Novaroli, G. B. Doulakas, M. Reist, B. Rolando, R. Fruttero, A. Gasco, and P. A. Carrupt. The lipophilicity behavior of three catechol-O-methyltransferase (COMT) inhibitors and simple analogues. *Helv. Chim. Acta* **89**:144–152 (2006).
105. U. Abshagen, G. Betzien, R. Endeke, B. Kaufmann, and G. Neugebauer. Pharmacokinetics and metabolism of isosorbide-dinitrate after intravenous and oral administration. *Eur. J. Clin. Pharmacol.* **27**:637–644 (1985).
106. V. Billard, P. L. Gambus, J. Barr, C. F. Minto, L. Corash, J. W. Tessman, J. L. Stickney, and S. L. Shafer. The pharmacokinetics of 8-methoxypsoralen following i.v. administration in humans. *Br. J. Clin. Pharmacol.* **40**:347–360 (1995).
107. M. G. Soars, B. Burchell, and R. J. Riley. *In vitro* analysis of human drug glucuronidation and prediction of *in vivo* metabolic clearance. *J. Pharmacol. Exp. Ther.* **301**:382–390 (2002).
108. A. Patel, P. M. Taylor, N. E. Wilsher, P. C. Butler, K. C. Ruparelia, and G. A. Potter. Use of an automated plate reader to measure partition coefficients. *J. Pharm. Pharmacol.* **57**:S–81 (2005).
109. J. W. Cheng, S. L. Charland, L. M. Shaw, S. Kobrin, S. Goldfarb, E. J. Stanek, and S. A. Spinler. Is the volume of distribution of digoxin reduced in patients with renal dysfunction? Determining digoxin pharmacokinetics by fluorescence polarization immunoassay. *Pharmacotherapy* **17**:584–590 (1997).
110. R. Kawai, D. Mathew, C. Tanaka, and M. Rowland. Physiologically based pharmacokinetics of cyclosporine A: extension to tissue distribution kinetics in rats and scale-up to human. *J. Pharmacol. Exp. Ther.* **287**:457–468 (1998).
111. B. Davies and T. Morris. Physiological parameters in laboratory animals and humans. *Pharm. Res.* **10**:1093–1095 (1993).
112. Y. Sakiya, Y. Tsuemura, Y. Sawada, M. Hanano, T. Marunaka, and Y. Umeno. Prediction of ftorafur disposition in rats and man by a physiologically based pharmacokinetic model. *Int. J. Pharm.* **25**:347–358 (1985).
113. J. Boon, R. M. Broekhuijs, P. Vanmunst, and E. Schretle. Abnormal pattern of phospholipids of plasma and erythrocytes in 4 children with obstructive jaundice with abnormal spontaneous hemolysis. *Clin. Chim. Acta* **23**:453 (1969).
114. T. E. Morgan, F. A. Short, and L. A. Cobb. Effect of long-term exercise on skeletal muscle lipid composition. *Am. J. Physiol.* **216**:82–86 (1969).
115. P. Poulin and K. Krishnan. A mechanistic algorithm for predicting blood:air partition coefficients of organic chemicals with the consideration of reversible binding in hemoglobin. *Toxicol. Appl. Pharmacol.* **136**:131–137 (1996).
116. L. Radulescu, C. Stancu, and F. Antohe. Antibodies against human oxidized low-density lipoprotein (LDL) as markers for human plasma modified lipoproteins. *Med. Sci. Monit.* **10**:BR207–BR214 (2004).
117. G. Sjogaard and B. Saltin. Extra- and intracellular water spaces in muscles of man at rest and with dynamic exercise. *Am. J. Physiol.* **243**:R271–R280 (1982).